

**X. Guo**

**A. Y. T. Leung<sup>1</sup>**

e-mail: bcaleung@cityu.edu.hk

Department of Building and Construction,  
City University of Hong Kong,  
Hong Kong, China

**H. Jiang**

Department of Mechanical and Aerospace  
Engineering,  
Arizona State University,  
Tempe, AZ 85287-6106

**X. Q. He**

Department of Building and Construction,  
City University of Hong Kong,  
Hong Kong, China

**Y. Huang**

Department of Mechanical and Industrial  
Engineering,  
University of Illinois at Urbana-Champaign,  
1206 West Green Street,  
Urbana, IL 61801

# Critical Strain of Carbon Nanotubes: An Atomic-Scale Finite Element Study

*This paper employs the atomic-scale finite element method (AFEM) to study critical strain of axial buckling for carbon nanotubes (CNTs). Brenner et al. "second-generation" empirical potential is used to model covalent bonds among atoms. The computed energy curve and critical strain for (8, 0) single-walled CNT (SWNT) agree well with molecular dynamics simulations. Both local and global buckling are achieved, two corresponding buckling zones are obtained, and the global buckling behavior of SWNT with a larger aspect ratio approaches gradually to that of a column described by Euler's formula. For double-walled CNTs with smaller ratio of length to outer diameter, the local buckling behavior can be explained by conventional shell theory very well. AFEM is an efficient way to study buckling of CNTs. [DOI: 10.1115/1.2198548]*

## Introduction

By atomic force microscope, Falvo et al. observed reversible high-strain deformation and periodic buckling of multiwalled carbon nanotubes (MWNT) [1]. Examining slices of MWNT embedded within a polymeric film by transmission electron microscopy, Lourie et al. reported experimental results of various deformation and fracture modes under compression [2]. To investigate buckling behavior of carbon nanotubes (CNTs), extensive theoretical research has been carried out. In general, the widely used theoretical methods can be divided into atomistic-based methods and continuum mechanics. Using molecular dynamics (MD), Yakobson et al. found that single-walled CNT (SWNT) switches into different morphological patterns when subject to large deformation [3]. Srivastava et al. investigated axial compression of SWNT using generalized tight-binding MD [4]. By MD simulation, Xiao et al. [5] and Liew et al. [6] studied instability of CNTs under axial compression, Sears and Batra [7] and Wang et al. [8] investigated critical strain for global and local buckling of CNTs, and further, Liew et al. [9] simulated the critical strain and buckling loads of CNT bundles. The atomistic-based methods are currently limited to very small length and time scales, due to insufficient computing power [6,9,10]. Several elasticity models can be comparatively easily used. Pantano et al. presented a nonlinear structural mechanics model and studied wrinkling of MWNT [11]. Based on explicit formula for the van der Waals (vdW) interaction

between any two layers of MWNT, He et al. established a shell buckling model [12] and Kitipornchai et al. studied buckling behavior of triple-walled CNTs embedded in an elastic matrix [13]. In the above continuum models, interatomic potential is not employed directly and multibody interactions cannot be considered accurately, so the behavior of discrete atoms and concrete configuration of CNT can hardly be achieved. Huang and his colleagues proposed a three-dimensional atomic-scale finite element method (AFEM) [14,15]. Using interatomic potential to consider the multibody interactions, AFEM is as accurate as molecular mechanics simulation. It is much faster than molecular mechanics because it uses the first and second order of derivative of total energy, while molecular mechanics employs the conjugate gradient method, which only uses its first order of derivative.

This paper employs AFEM to study critical strain of axial buckling for CNTs. The achieved energy curve and critical strain for (8, 0) SWNT agree well with recent MD simulations, which verifies the application of AFEM to study buckling of CNTs. It is found that there are two kinds of buckling: local and global. With the aspect ratio (ratio of length to diameter) increasing, CNTs first locally buckle and then globally buckle. The local and global buckling zones can be searched in detail, and the critical strain shows different characteristics in two zones. The global buckling behavior of SWNT with a larger aspect ratio can be explained by Euler's buckling formula for column. For double-walled CNTs (DWNTs) with smaller ratio of length to outer diameter, the local buckling behavior is consistent with conventional shell theory.

## Potential Function and AFEM for CNTs

As for the CNTs, covalent bonds among atoms can be modeled according to Brenner et al. "second-generation" empirical potentials [16]. For SWNT, covalent bonds are dominant interaction, so in the following simulations on SWNT, vdW interaction is not considered. For MWNT, vdW interaction is expressed according

<sup>1</sup>Author to whom correspondence should be addressed.

Contributed by the Applied Mechanics Division of ASME for publication in the JOURNAL OF APPLIED MECHANICS. Manuscript received September 30, 2005; final manuscript received February 22, 2006. Review conducted by R. M. McMeeking. Discussion on the paper should be addressed to the Editor, Prof. Robert M. McMeeking, Journal of Applied Mechanics, Department of Mechanical and Environmental Engineering, University of California—Santa Barbara, Santa Barbara, CA 93106-5070, and will be accepted until four months after final publication of the paper itself in the ASME JOURNAL OF APPLIED MECHANICS.

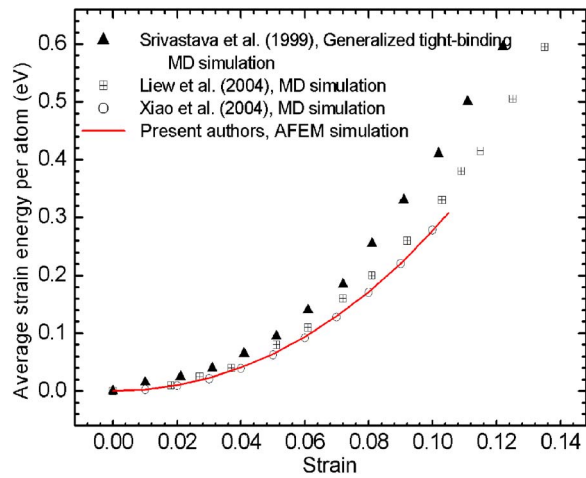


**Fig. 1 Comparison among the strain energy curves for (8, 0) SWNT**

to the Lennard-Jones 12-6 model [17] and is taken as a nonlinear spring when the distance between two carbon atoms in the different layer is less than the cutoff radius.

In AFEM for CNTs proposed by Huang and his colleagues [14,15], the AFEM element consists of ten atoms because each carbon atom has three nearest-neighboring atoms and six second nearest-neighboring atoms. A schematic diagram of AFEM element, the associated element stiffness matrix, and the nonequilibrium force vector are therein [14,15]. Such an element captures the interactions among the central atom and other atoms. The number of nonzero entries in the global stiffness matrix  $K$  is of order  $N$ , so is the computational effort to solve  $Ku=P$ , while the conjugate gradient method widely used in atomistic studies is of order  $N^2$ .

### Simulation on Buckling of CNTs

Consider an initial equilibrium configuration of CNT. Unless direct specification, one end of the CNT is fixed and the in-plane displacements of the other end are prohibited in our paper. An axial displacement can be applied to compress it, and AFEM can be performed to obtain new equilibrium configuration; then a further displacement can be applied. It deforms linearly when the strain is small. With the strain increasing, the stiffness matrix will lose positive definiteness at a certain point, which is the critical strain for axial buckling. The post-buckling configuration of CNT can also be achieved. All calculation is performed by ABAQUS via its UEL subroutine [18].

First, we study axial buckling of a (8, 0) zigzag SWNT, with length 4.07 nm and diameter 0.63 nm. The average strain energy per atom is calculated as the difference in the average energy per atom in the strained and unstrained system as a function of strain shown in Fig. 1. In Srivastava et al. [4], its structural deformation strained at 0.12 in the generalized tight-binding MD is completely spontaneous and leads to plastic collapse. By MD simulation using Brenner et al. "second-generation" empirical potential, Xiao et al. investigated nonlinear elastic properties and instability of SWNT under axial compression and found that (8, 0) SWNT can deform elastically to the strain 0.10 [5], while Liew et al. have shown that it can be compressed up to a strain 0.135 before buckling [6]. In our AFEM simulation, the critical strain is 0.105. For comparison, the strain energy curves of Srivastava et al. [4], Xiao et al. [5], and Liew et al. [6] are compared in Fig. 1. It can be easily found that our energy curve approaches theirs closely. Especially, the energy curve of Xiao et al. and ours almost coincide with each other. Srivastava et al. used the tight-binding MD scheme of Menon et al. [19], resulting in the highest strain energy in comparison to the others. Although the same Brenner et al.

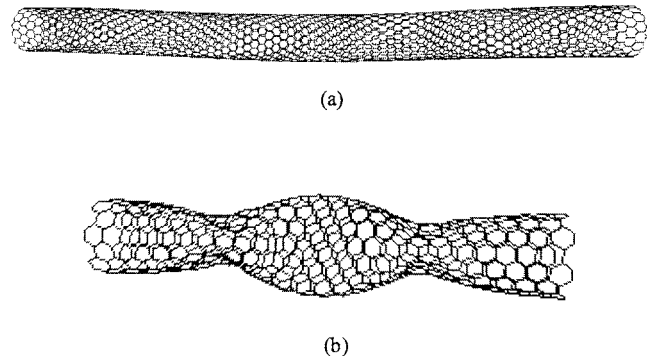
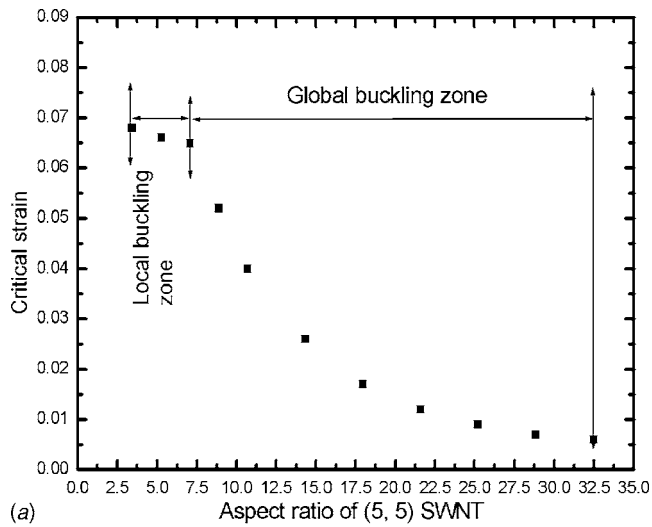


**Fig. 2 (a) Morphology of (16, 0) SWNT after global buckling, (b) morphology of (7, 7) SWNT after local buckling. Two kinds of buckling for CNTs with different aspect ratios.**

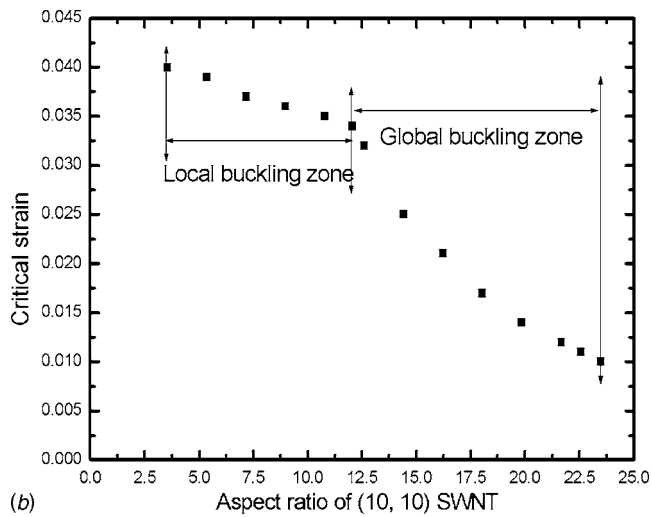
potential was employed in Liew et al., that their SWNT is a bit longer explains the slight difference. Thus, the application of AFEM to study the critical strain of axial buckling for CNTs is verified. The time needed really depends on the applied total displacement step size and the initial step size. Here only tens of seconds are needed to achieve the final critical strain 0.105. To show the effect of the boundary condition on the buckling behavior, we still keep one end of the (8, 0) SWNT fixed, but allow for the in-plane displacement at the other end. It is found that the new boundary conditions almost do not affect the strain energy, but reduce the critical strain to 0.03, less than one-third of the former one. The phenomenon that the release of the constraint will facilitate the buckling is consistent with the continuum mechanics.

As for CNT, there are two kinds of buckling. The first one is column buckling, where CNT approximately keeps the circular cross section and buckles sideways as a whole. The second one is shell buckling, where CNT buckles with lobes and half waves along the tube and the axis remains straight. It was the same with Wang et al. [8], the former and latter is named the global buckling and local buckling, respectively. For a (16, 0) zigzag SWNT, with length 17.1 nm and diameter 1.254 nm, by MD simulation, Sears and Batra found that critical strain is 0.02784 and it is global buckling [7]. In our AFEM simulation, its critical strain is 0.029, which represents 4.2% relative error with theirs, and it is also global buckling, shown in Fig. 2(a) [20]. In our AFEM simulation on a (7, 7) armchair SWNT, with length 6 nm and diameter 0.95 nm under axial compression, there is local buckling in good agreement with MD simulation of Jakobson et al. [3]. Its morphology after buckling is shown in Fig. 2(b) [20].

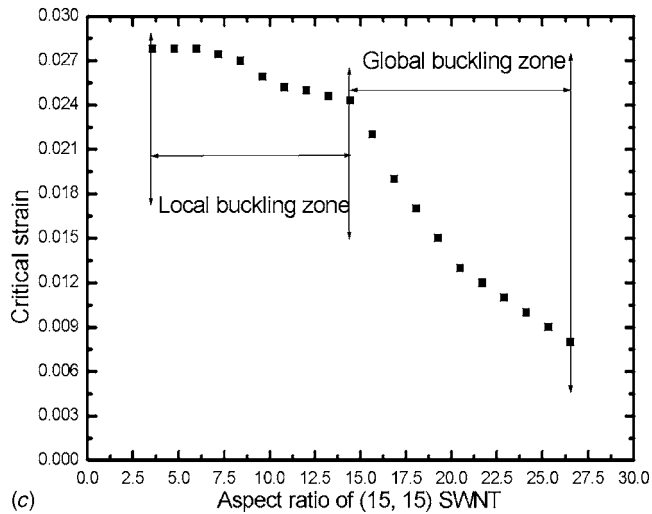
Figure 3 shows the various critical strains  $\epsilon_{cr}$  of (5, 5), (10, 10), and (15, 15) armchair SWNTs at different length  $l$ , while their aspect ratios change from  $<5$  to  $>20$ . It is obvious that the shorter SWNTs buckle locally and the longer ones buckle globally. There is an inflexion point in each curve of Fig. 3, and the aspect ratio is 7.1, 12.0, and 14.4, while the corresponding length is 4.788 nm, 16.35 nm, and 29.39 nm, respectively. With the diameter increasing, the length associated with inflexion point increases and so does the local buckling zone. The MD simulation of Wang et al. shows the length associated with its inflexion point for (10, 10) SWNT is 15.79 nm [8], and the result in our AFEM simulation has  $<4\%$  relative error with theirs. In the local buckling zone, the critical strain decreases very slowly. In the global buckling zone, the critical strain first decreases fast, and then decreases slowly when the length is comparatively larger, which is consistent with MD simulation of Liew et al. [6]. Thus, to show this important characteristic of critical strain in the global buckling zone, the exponential decay function is chosen to fit the corresponding data, i.e.,



(a)



(b)

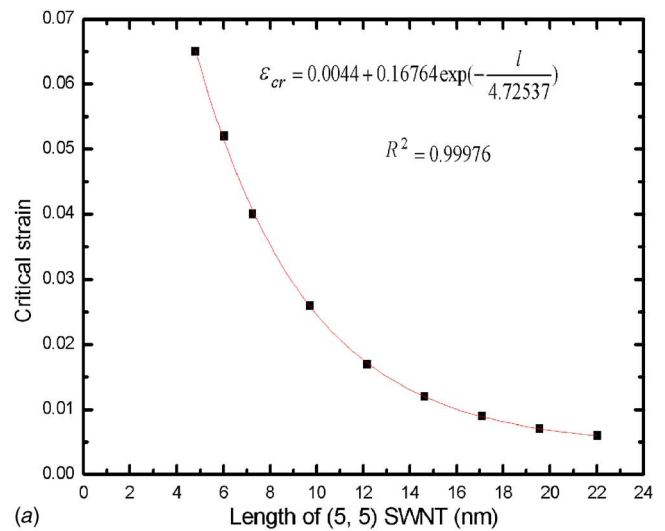


(c)

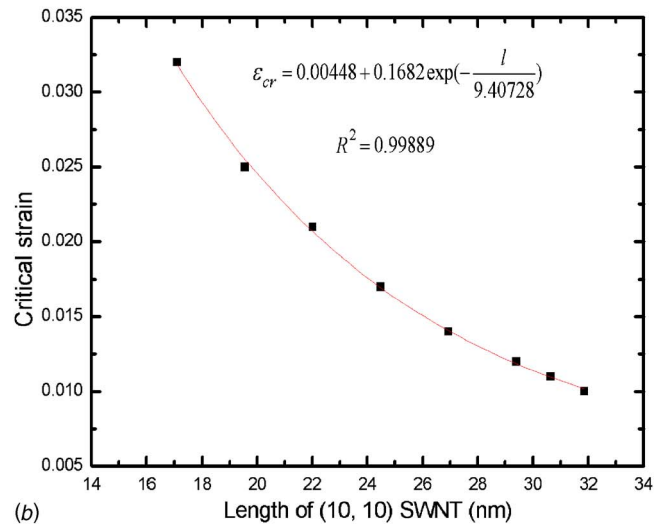
**Fig. 3** Critical strain versus aspect ratio for (a) (5, 5) SWNT with diameter of 0.678 nm, (b) (10, 10) SWNT with diameter of 1.357 nm, and (c) (15, 15) SWNT with diameter of 2.036 nm

$$\varepsilon_{cr} = C + A \exp\left(-\frac{l}{B}\right) \quad (1)$$

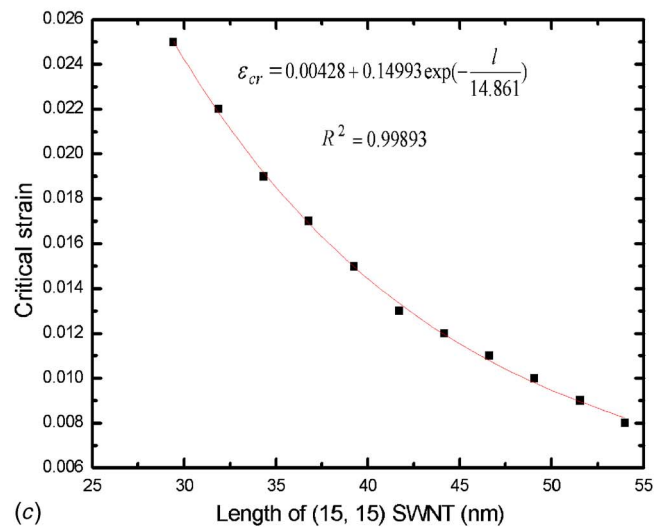
where  $A$ ,  $B$ , and  $C$  are fitting parameters.  $1/B$  shows the decay of critical strain  $\varepsilon_{cr}$  with the length  $l$ , so it is named as decay rate.



(a)



(b)



(c)

**Fig. 4** Critical strain and fitting result by Eq. (1) for global buckling of (a) (5, 5), (b) (10, 10), and (c) (15, 15) SWNTs with different length

The fitting curves and the associated correlation coefficients are shown in Fig. 4. From Fig. 4, it can be found that Eq. (1) fits the data very well. With the diameter increasing,  $B$  increases, and so

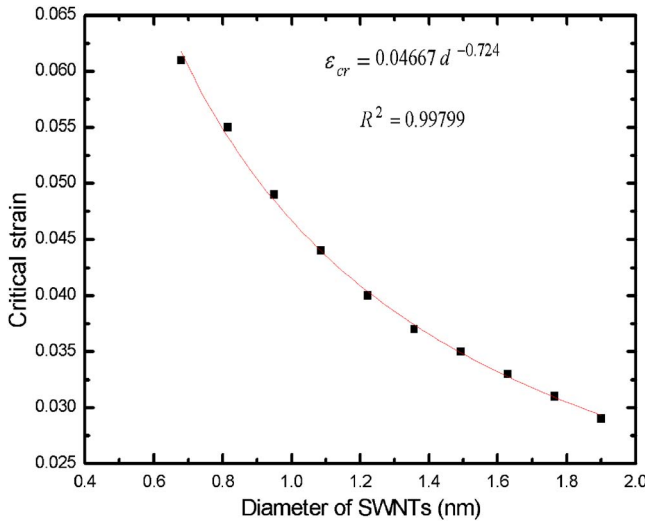


Fig. 5 Critical strain versus the diameter of SWNT with approximate aspect ratio of 7.6

the decay rate decreases, which is because, for SWNT with larger diameter, more length is needed to realize the same change of aspect ratio.

As shown in Fig. 2(a), the morphology of CNT after global buckling is similar to the buckled column, and quantitative discussion on the critical strain is performed as follows. According to Euler's formula, the critical strain  $\epsilon_{cr}$  of column with both ends built in is given by [21]

$$\epsilon_{cr} = \frac{4\pi^2 I}{Al^2} \quad (2)$$

where  $A$  is the cross-sectional area and  $I$  is moment of inertia of the column. Equation (2) shows that the critical strain  $\epsilon_{cr}$  will be inversely proportional to the square of the length, given the constant  $A$  and  $I$ . As shown in Fig. 3, the data associated with global buckling are the right part of whole curve; thus, a power function with a shift term is chosen to fit the data in Fig. 4, i.e.,

$$\epsilon_{cr} = al^b + c \quad (3)$$

where  $a, b, c$  are fitting parameters. It is found that Eq. (3) can also fit each curve in Fig. 4 very well and all correlation coefficients are larger than 0.997.  $b$  is  $-1.01412$ ,  $-1.44938$ , and  $-1.62841$ ; thus, the critical strain  $\epsilon_{cr}$  is linearly related to the length to power of  $-1.01412$ ,  $-1.44938$ , and  $-1.62841$  for (5, 5), (10, 10), and (15, 15) SWNT, respectively. With the diameter increasing, number of the atoms in each circumference increase, and  $b$  approaches to  $-2.0$  gradually, which shows that the global buckling behavior of SWNT with a larger aspect ratio approaches gradually to that of a column described by Euler's formula.

For armchair SWNTs with an approximate fixed aspect ratio 7.6, the relationship between critical strain in our AFEM simulation and the diameter is shown in Fig. 5. From Fig. 5, it is observed that as the diameter increases, the critical strain decreases. The power function is used to fit the critical strain, and it is found that the critical strain is inversely proportional to the diameter to power of 0.724.

Finally, we employ AFEM to study buckling behavior of DWNTs. They are (5, 5) and (10, 10), (10, 10) and (15, 15), (15, 15) and (20, 20), (20, 20) and (25, 25), (25, 25) and (30, 30), sequentially. The ratio of length to the corresponding outer diameter is kept as  $\sim 4.5$ . Their critical strain  $\epsilon_{cr}$  versus the outer diameter is shown in Fig. 6. It shows that as the length increases, the critical strain decreases. As shown in Fig. 2(b), the morphology of CNT after local buckling is similar with the buckled thin shell,

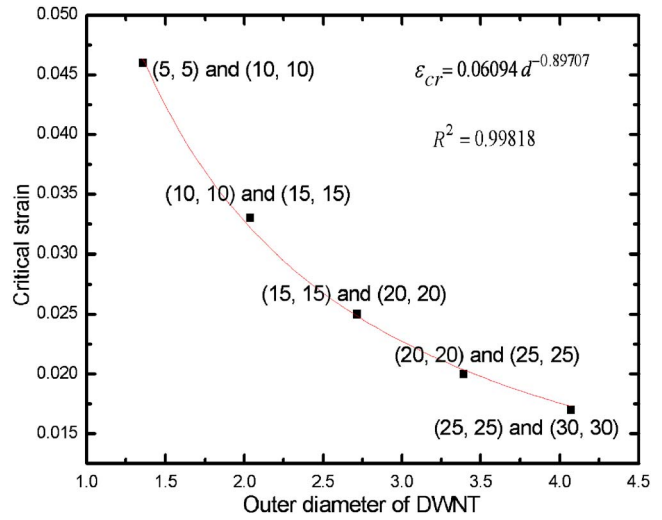


Fig. 6 Critical strain versus the outer diameter of DWNT. The ratio of length to the corresponding outer diameter is kept as  $\sim 4.5$

and quantitative discussion on the critical strain is performed as follows. For the buckling of a compressed thin shell, the critical strain is [21]

$$\epsilon_{cr} = \frac{2h}{d\sqrt{3(1-\nu^2)}}\alpha \quad (\alpha = 0.6 - 1) \quad (4)$$

where  $h$  is the effective thickness,  $d$  is the diameter of the shell,  $\nu$  is the Poisson's ratio, and  $\alpha$  is correction coefficient. Usually,  $\alpha = 1$  if it buckles into short longitudinal waves, otherwise it decreases with longer waves. Equation (4) shows that the critical strain will be inversely proportional to the diameter  $d$ , given constant effective thickness  $h$ . The fitting results on MD simulation of Xiao et al. [5] also reach that same conclusion on the critical strain for shorter SWNTs. Because the ratio of length to the corresponding outer diameter keeps constant, we fit the critical strain with the length in Fig. 6 and found that the critical strain is inversely proportional to the length to power of 0.897. There are different definitions of effective thickness of CNTs [3,11,22–24]. In our above analysis, the effective thickness of different DWNT is assumed as a constant and the DWNT is taken as thin shell. Further considering the vague definition on the diameter of DWNT, the buckling behavior of DWNTs with a smaller ratio of length to outer diameter can be explained very well by the conventional shell theory.

In order to show the effect of the intertube vdW interaction, we study the buckling of the above (5, 5) and (10, 10) DWNT without intertube vdW interaction. It is found that it does not affect the strain energy, but reduces the critical strain to 0.04, which is 15% smaller than the former one. The attractive intertube vdW interaction explains the larger critical strain when the vdW interaction is considered.

## Conclusions

This paper employs the atomic-scale finite element method (AFEM) to study critical strain of the axial buckling for SWNTs and DWNTs. Comparison of the energy curve and critical strain for (8, 0) SWNT with MD simulations validates the application of AFEM. There are two kinds of buckling: local and global. With the aspect ratio increasing, SWNT first locally buckles and then globally buckles. With its diameter increasing, the length associated with inflexion point increases, decay rate of critical strain with length in the global buckling zone slows down, and its global buckling behavior gradually approaches that of a column described by Euler's formula. The relationship between critical

strain and the diameter for armchair SWNTs with an approximate fixed aspect ratio is obtained. For DWNTs with smaller ratio of length to outer diameter, the dependence of the critical strain on diameter is explained by conventional shell theory very well. AFEM is much faster in terms of computation because it is within the theoretical framework of the conventional FEM. It is an efficient way to study buckling of CNTs.

### Acknowledgment

The research is supported by City University of Hong Kong Grant No. SRG7001824.

### References

- [1] Falvo, M. R., Clary, G. J., Taylor, R. M., II, Chi, V., Brooks, F. P., Jr., Washburn, S., and Superfine, R., 1997, "Bending and Buckling of Carbon Nanotubes Under Large Strain," *Nature (London)*, **389**, pp. 582–584.
- [2] Lourie, O., Cox, D. M., and Wagner, H. D., 1998, "Buckling and Collapse of Embedded Carbon Nanotubes," *Phys. Rev. Lett.*, **81**, pp. 1638–1641.
- [3] Yakobson, B. I., Brabec, C. J., and Bernholc, J., 1996, "Nanomechanics of Carbon Tubes: Instabilities Beyond Linear Response," *Phys. Rev. Lett.*, **76**, pp. 2511–2514.
- [4] Srivastava, D., Menon, M., and Cho, K., 1999, "Nanoplasticity of Single-Wall Carbon Nanotubes Under Uniaxial Compression," *Phys. Rev. Lett.*, **83**, pp. 2973–2976.
- [5] Xiao, T., Xu, X., and Liao, K., 2004, "Characterization of Nonlinear Elasticity and Elastic Instability in Single-Walled Carbon Nanotubes," *J. Appl. Phys.*, **95**, pp. 8145–8148.
- [6] Liew, K. M., Wong, C. H., He, X. Q., Tan, M. J., and Meguid, S. A., 2004, "Nanomechanics of Single and Multiwalled Carbon Nanotubes," *Phys. Rev. B*, **69**, p. 115429.
- [7] Sears, A., and Batra, R. C., 2004, "Macroscopic Properties of Carbon Nanotubes From Molecular-Mechanics Simulations," *Phys. Rev. B*, **69**, p. 235406.
- [8] Wang, Y., Wang, X. X., Ni, X. G., and Wu, H. A., 2005, "Simulation of the Elastic Response and the Buckling Modes of Single-Walled Carbon Nanotubes," *Comput. Mater. Sci.*, **32**, pp. 141–146.
- [9] Liew, K. M., Wong, C. H., and Tan, M. J., 2006, "Tensile and Compressive Properties of Carbon Nanotube Bundles," *Acta Mater.*, **54**, pp. 225–231.
- [10] Liew, K. M., He, X. Q., and Wong, C. H., 2004, "On the Study of Elastic and Plastic Properties of Multi-Walled Carbon Nanotubes Under Axial Tension Using Molecular Dynamics Simulation," *Acta Mater.*, **52**, pp. 2521–2527.
- [11] Pantano, A., Parks, D. M., and Boyce, M. C., 2004, "Mechanics of Deformation of Single- and Multi-Wall Carbon Nanotubes," *J. Mech. Phys. Solids*, **52**, pp. 789–821.
- [12] He, X. Q., Kitipornchai, S., and Liew, K. M., 2005, "Buckling Analysis of Multi-Walled Carbon Nanotubes: A Continuum Model Accounting for van der Waals Interaction," *J. Mech. Phys. Solids*, **53**, pp. 303–326.
- [13] Kitipornchai, S., He, X. Q., and Liew, K. M., 2005, "Buckling Analysis of Triple-Walled Carbon Nanotubes Embedded in an Elastic Matrix," *J. Appl. Phys.*, **97**, p. 114318.
- [14] Liu, B., Huang, Y., Jiang, H., Qu, S., and Hwang, K. C., 2004, "The Atomic-Scale Finite Element Method," *Comput. Methods Appl. Mech. Eng.*, **193**, pp. 1849–1864.
- [15] Liu, B., Jiang, H., Huang, Y., Qu, S., Yu, M. F., and Hwang, K. C., 2005, "Atomic-Scale Finite Element Method in Multiscale Computation With Applications to Carbon Nanotubes," *Phys. Rev. B*, **72**, p. 035435.
- [16] Brenner, D. W., Shenderova, O. A., Harrison, J. A., Stuart, S. J., Ni, B., and Sinnott, S. B., 2002, "A Second-Generation Reactive Empirical Bond Order (Rebo) Potential Energy Expression for Hydrocarbons," *J. Phys.: Condens. Matter*, **14**, pp. 783–802.
- [17] Girifalco, L. A., Hodak, M., and Lee, R. S., 2000, "Carbon Nanotubes, Buckyballs, Ropes, and a Universal Graphitic Potential," *Phys. Rev. B*, **62**, pp. 13104–13110.
- [18] ABAQUS, *ABAQUS Theory Manual and Users Manual*, 2002, version 6.2, Hibbit, Karlsson and Sorensen Inc., Pawtucket, RI.
- [19] Menon, M., Richter, E., and Subbaswamy, K. R., 1996, "Structural and Vibrational Properties of Fullerenes and Nanotubes in a Nonorthogonal Tight-Binding Scheme," *J. Chem. Phys.*, **104**, pp. 5875–5882.
- [20] Humphrey, W., Dalke, A., and Schulten, K., 1996, "VMD—Visual Molecular Dynamics," *J. Mol. Graphics*, **14**, pp. 33–38.
- [21] Timoshenko, S. P., and Gere, J. M., 1961, *Theory of Elastic Stability*, 2nd ed., McGraw-Hill, New York.
- [22] Zhou, X., Zhou, J. J., and Ou-Yang, Z. C., 2000, "Strain Energy and Young's Modulus of Single-Wall Carbon Nanotubes Calculated From Electronic Energy-Band Theory," *Phys. Rev. B*, **62**, pp. 13692–13696.
- [23] Kundin, K. N., Scuseria, G. E., and Yakobson, B. I., 2001, "C<sub>2</sub>F, BN, and C Nanoshell Elasticity From Ab Initio Computations," *Phys. Rev. B*, **64**, p. 235406.
- [24] Tu, Z. C., and Ou-Yang, Z. C., 2002, "Single-Walled and Multiwalled Carbon Nanotubes Viewed as Elastic Tubes With the Effective Young's Moduli Dependent on Layer Number," *Phys. Rev. B*, **65**, p. 233407.